Serine Protease of Hepatitis C Virus Expressed in Insect Cells as the NS3/4A Complex

Dasa Lipovsek Sali,*,‡,§ Richard Ingram,‡ Michele Wendel,‡ Divya Gupta,‡ Charles McNemar,‡ Anthony Tsarbopoulos,‡ Janice W. Chen,|| Zhi Hong,|| Robert Chase,|| Christine Risano,|| Rumin Zhang,‡ Nanhua Yao,‡ Ann D. Kwong,||,⊥ Lata Ramanathan,‡ Hung V. Le,‡ and Patricia C. Weber‡

Departments of Structural Chemistry and Antiviral Chemotherapy, Schering-Plough Research Institute, 2015 Galloping Hill Road, Kenilworth, New Jersey 07033

Received August 13, 1997; Revised Manuscript Received November 14, 1997

ABSTRACT: Hepatitis C virus (HCV) protease NS3 and its protein activator NS4A participate in the processing of the viral polyprotein into its constituent nonstructural proteins. The NS3/4A complex is thus an attractive target for antiviral therapy against HCV. We expressed the full-length NS3 and NS4A in insect cells as a soluble fusion protein with an N-terminal polyhistidine tag and purified the two proteins to homogeneity. Cleavage at the junction between HisNS3 and NS4A occurs during expression, producing a noncovalent complex between HisNS3 and NS4A with a subnanomolar dissociation constant. We purified the HisNS3/4A complex by detergent extraction of cell lysate and by metal chelate chromatography. We removed the His tag by thrombin cleavage and then further purified the complex by gel filtration. The purified NS3/4A complex is active in a protease assay using a synthetic peptide substrate derived from the NS5A−NS5B junction, with k_{cat}/K_m of 3700 (± 600) M^{-1} s^{-1}, an order of magnitude above those previously reported for NS3 expressed by other strategies. This high protease activity implies that the full-length sequences of NS3 and NS4A are required for optimal activity of the NS3 protease domain. We examined the dependence of the NS3/4A protease activity on buffer conditions, temperature, and the presence of detergents. We find that, under most conditions, NS3 protease activity is dependent on the aggregation state of the NS3/4A complex. The monodisperse, soluble form of the NS3/4A complex is associated with the highest protease activity.

Hepatitis C virus (HCV)[1] is the major cause of transfusion-associated and community-acquired non-A, non-B hepatitis worldwide *(1)*. Chronic HCV infection is associated with liver cirrhosis and hepatocellular carcinoma *(2)*. Currently, HCV infection is treated with α-interferon, which is only effective in approximately 25% of patients (*3*). A vaccine against HCV has yet to be developed, and more effective therapeutic agents are needed.

The HCV genome has been cloned and sequenced (*4*−*8*). The sequencing data reveals that HCV is a single-stranded, positive-sense RNA virus that belongs to the family Flaviviridae (*9*). The genome encodes a single polyprotein of approximately 3000 amino acid residues in the order of NH_2-C-E1-E2-p7-NS2-NS3-NS4A-NS4B-NS5A-NS5B-COOH. The polyprotein is processed by host and viral proteases. The host signal peptidases cleave the polyprotein at the junctions between the structural proteins C, E1, and E2 (*10*). Processing at the NS2/3 junction is an intramolecular (cis) cleavage that requires the C-terminal domain of NS2 and the N-terminal domain of NS3 protein. The viral serine protease located in the N-terminal domain of NS3 cleaves at the remaining junctions in the nonstructural region of the polyprotein, including the cis cleavage between a threonine and a serine residue at the NS3−NS4A junction and the trans cleavages between cysteine and serine residues at the NS4A−NS4B, NS4B−NS5A, and NS5A−NS5B junctions *(11)*. The C-terminal domain of NS3 has both NTPase and helicase activities *(12, 13)*. The NS4A protein is an activator of the NS3 protease activity, with the degree of stimulation dependent on the location of the cleavage site *(11, 14)*.

Three-dimensional structures of the N-terminal, 181 residue protease domain of NS3, both by itself *(15)* and in complex with an NS4A-derived peptide of 19 amino acid residues *(16)*, were recently determined by X-ray crystal-

* To whom correspondence should be addressed.
‡ Department of Structural Chemistry.
§ Present address: Phylos, Inc., 300 Putnam Ave., Cambridge, MA 02139. Telephone: (617) 491-0077. Fax: (617) 491-9494.
|| Department of Antiviral Chemotherapy.
⊥ Present address: Vertex Pharmaceuticals, Inc., 130 Waverly St., Cambridge, MA 02139.

[1] Abbreviations: ATP, adenosine triphosphate; BSA, bovine serum albumin; CAPS, 3-(cyclohexylamino)-1-propanesulfonic acid; CD, circular dichroism; CHAPS, 3-[(3-cholamidopropyl)dimethylammonio]-1-propanesulfonate; CHES, 2-(cyclohexylamino)ethanesulfonic acid; CMC, critical micelle concentration; DTT, dithiothreitol; ECL, enhanced chemiluminescence; EDTA, ethylenediaminetetraacetic acid; GTP, guanosine triphosphate; HCV, hepatitis C virus; HEPES, *N*-(2-hydroxyethyl)piperazine-*N*′-2-ethanesulfonic acid; HPLC, high-performance liquid chromatography; IC_{50}, inhibitor concentration for 50% inhibition; MALDI, matrix-assisted laser desorption/ionization; MES, 2-(*N*-morpholino)ethanesulfonic acid; moi, multiplicity of infection; MOPS, 3-(*N*-morpholino)propanesulfonic acid; Ni−NTA, nickel−nitrilotriacetic acid; NS, nonstructural protein; NTP, nucleoside triphosphate; PAGE, polyacrylamide gel electrophoresis; PIPES, 1,4-piperazinediethanesulfonic acid; PMSF, phenylmethanesulfonyl fluoride; PolyU, poly(uridylic acid); SDS, sodium dodecyl sulfate; Sf9, *Spodoptera frugiperda;* TFA, trifluoroacetic acid; Tris, tris(hydroxymethyl)aminomethane; Tween-20, poly(oxyethylene)sorbitan monolaurate; UV, ultraviolet.

S0006-2960(97)02010-2 CCC: $15.00
Published on Web 02/18/1998

lography, revealing a chymotrypsin-like fold and a structural zinc-binding site. The crystal structure of the C-terminal, 451-residue helicase domain of NS3 has also been determined *(17)*. In contrast, structural studies of the full-length NS3 (631 residues) and NS4A (54 residues) have been hampered by difficulties in obtaining sufficient amounts of soluble and pure enzyme. The only report of NS3/4A expression to date *(18)*, which used transiently transfected COS cell culture, describes a yield of 1−3 μg of 85% pure NS3/4A/10^7 cells and the activity of NS3/4A in an in vitro transcription/translation protease assay as well as in NTPase and helicase assays.

Here we report the use of an Sf9/baculovirus system to express the full-length NS3/4A complex, which includes both the N-terminal protease domain and the C-terminal helicase domain of NS3, as well as the full-length NS4A. We describe the procedure employed to purify the NS3/4A complex to homogeneity at milligram levels, as well as the characterization of its enzymatic and biophysical properties. In particular, we have confirmed and quantitated the NTPase and helicase activities, optimized the protease reaction conditions, and examined the relation between the aggregation state and the protease activity of NS3/4A.

EXPERIMENTAL PROCEDURES

Materials. *n*-Dodecyl β-D-maltoside was obtained from Anatrace (Maumee, OH). Nonidet P-40 was obtained from Calbiochem (La Jolla, CA). Ni−NTA agarose resin was obtained from Qiagen (Chatsworth, CA). Human thrombin was obtained from Enzyme Research Laboratories, Inc. (South Bend, IN). The ECL Western detection kit was obtained from Amersham (Arlington Heights, IL). All reagents for the N-terminal peptide sequencer were purchased from Applied Biosystems, except for the phenylthiohydantoin (PTH) standards, which were from Hewlett-Packard (G2013A). Argon (99.999%) and nitrogen (99.9999%) were supplied from SOS Gases. Fmoc-amino acids were purchased from Applied Biosystems (Foster City, CA) and Novabiochem (San Diego, CA). All NTPs, 7mGpppG, and poly(uridylic acid) (polyU) were purchased from Boehringer Mannheim. [γ-^{32}P]ATP and [α-^{32}P]GTP were obtained from Amersham Corp. SP6 RNA polymerase was purchased from Promega (Madison, WI) and RNase Block was obtained from Stratagene (La Jolla, CA). PEI−cellulose F precoated plastic TLC plates for the ATPase assay were obtained from EM Separations Technology (Gibbstown, NJ). Streptavidin-coated FlashPlates for the 96-well plate helicase assay were obtained from New England Nuclear (Boston, MA).

Cloning of NS3/4A and Preparation of High-Titer Baculovirus Stock. The full-length natural sequences of NS3 and NS4A proteins, as well as the 16 N-terminal residues of NS4B, of the HCV H/1a strain (originally obtained from Charles M. Rice, Washington University at St. Louis) *(11)*, were cloned in tandem into the pAcHLT-B baculovirus expression vector (PharMingen, San Diego, CA) between the *Eco*RI and *Bgl*II restriction sites (unpublished data). The vector sequence included a region encoding a 53-residue N-terminal leader sequence, which contained a hexahistidine tag. The resulting HisNS3/4A construct (Figure 1) was transfected into Sf9 cells, the recombinant virus was plaque-purified, and a high-titer virus stock was grown and titered by Invitrogen Custom Baculovirus Division (San Diego, CA).

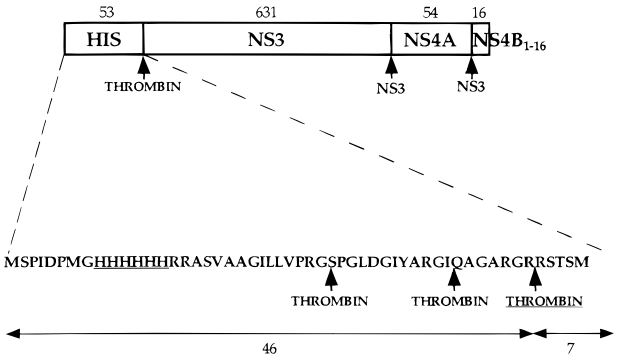

FIGURE 1: HisNS3/4A construct expressed in the baculovirus/Sf9 system. HIS, 53-residue leader sequence containing a hexahistidine tag. The expanded region shows the entire sequence of the leader peptide and the sites within the leader peptide where thrombin cleavage has been observed. NS3, 631-residue NS3 protease/helicase. NS4A, 54-residue NS4A peptide. Protease recognition sites cleaved by thrombin and NS3/4A protease itself are shown by arrows. The underlined thrombin cleavage site was where the majority of HisNS3/4A was cleaved under the conditions used during the purification procedure (50 units/mg of protein).

Expression and Purification of NS3/4A. A 5 L Sf9 cell culture was started at 5×10^5 cells/mL in Bio-Whittaker Insect X-PRESS medium and grown for 72 h at 27 °C, then diluted with an equal volume of fresh Bio-Whittaker Insect X-PRESS medium and grown for another 24 h. When the Sf9 culture reached approximately 2×10^6 cells/mL, the culture was infected with the HisNS3/4A high-titer baculovirus stock at an moi of 0.5. The infected culture was harvested 48 h later by centrifugation at 1000*g* and 4 °C. All further manipulation and purification procedures were performed at 4 °C.

The cell pellet from a 10 L fermentation was homogenized and resuspended in /1400 mL of buffer A (50 mM sodium phosphate, pH 8.0, 0.3 M NaCl, 10 mM β-mercaptoethanol, 10% glycerol, 100 ng/mL leupeptin, and 200 ng/mL antipain) containing 0.05% *n*-dodecyl β-D-maltoside. The homogenate was ultracentrifuged at 100000*g*; the pellet was resuspended in 1400 mL of buffer B (0.5% *n*-dodecyl β-D-maltoside in buffer A), homogenized, and again ultracentrifuged at 100000*g*. The supernatant obtained by the second ultracentrifugation was batch-adsorbed for 1 h at 4 °C onto 40 mL of Qiagen Ni−NTA metal chelate resin that had been equilibrated with buffer A. The resin was packed into a column, which ran by gravity at 0.5−3 mL/min. The Ni−NTA−agarose column was washed with 20 column volumes of buffer C (0.05% *n*-dodecyl β-D-maltoside in buffer A) and 10 column volumes of buffer D (50 mM imidazole in buffer C). HisNS3/4A was eluted with 10 column volumes of buffer E (250 mM imidazole in buffer C).

The leader peptide was removed from Ni−NTA-purified HisNS3/4A by cleavage with 50 NIH units of human thrombin/mg of HisNS3/4A for 18 h at 4 °C. The cleaved NS3/4A was separated from the leader peptide, thrombin, and aggregated NS3/4A by gel filtration on a HiLoad 26/60, Superdex 200 pg column (Pharmacia), which was preequilibrated in buffer C and eluted at 2 mL/min. The fractions containing NS3/4A but no thrombin were identified by Western blot analysis using rabbit antisera against NS3 and NS4A *(19)* or sheep antisera against thrombin and the ECL detection system (Amersham). The fractions containing the purified NS3/4A were pooled and stored at −80 °C, then

thawed and concentrated in an Amicon 8MC microultrafiltration system with a 25 mm YM30 membrane to the desired concentration immediately before use. Throughout the purification, the purity of the sample was monitored by SDS−PAGE and densitometry on an LKB Ultroscan XL laser densitometer.

Determination of Protein Concentration. The extinction coefficient for purified NS3/4A was determined by amino acid analysis and UV spectroscopy of the protein sample in 25 mM HEPES, pH 8.0, 0.5 M NaCl, 10 mM dithiothreitol, and 0.01% *n*-dodecyl β-D-maltoside. Vapor phase hydrolysis of the sample was carried out for 1 h at 150 °C in 6 M HCl, using a Waters Pico-Tag workstation. The amino acid analysis was accomplished using a Hewlett-Packard Aminoquant II OPA/Fmoc system. Protein concentration of NS3/4A samples determined by the above method was used to calibrate a Bio-Rad protein assay, which was used routinely during the purification procedure.

N-Terminal Amino Acid Sequence Determination. Sequence analysis was performed on an Applied Biosystems 477A pulsed-liquid sequencer combined with an Applied Biosystems 120A PTH analyzer. The thrombin-cleaved NS3/4A sample was separated by SDS−PAGE and transferred onto a PVDF membrane, and the NS3 band was excised for analysis. The Superdex-200 purified NS3/4A was applied to PVDF using the Applied Biosystems ProSpin system to remove the glycerol from the sample. Both samples were sequenced for 10 cycles on the sequencer.

Mass Spectrometry. Matrix-assisted laser desorption/ionization (MALDI) mass spectra were obtained on a PerSeptive Voyager RP reflector-type time-of-flight mass spectrometer equipped with a nitrogen laser (wavelength 337 nm). Mass measurement of the NS3/4A samples was performed in the linear mode using super-dihydroxybenzoic acid (sDHB) for the matrix, as described previously *(20)*. The NS3/4A samples analyzed were concentrated to 1−4 mg/mL in 25 mM HEPES, pH 8.0, 0.5 M NaCl, 10 mM dithiothreitol, and 0.01% *n*-dodecyl β-D-maltoside. Matrix solution (10 μL) was added to 1 μL of the protein solution; 0.5−1 μL of the resulting mixture was applied onto the sample plate and air-dried prior to its transfer into the source of the mass spectrometer.

Peptide Synthesis. The P8P8′K substrate peptide derived from the HCV (H/1a) 5A/5B junction, DTEDVVCCSMSYTWTGK (5AB peptide) was synthesized from a preloaded Wang resin on an automated ABI model 431A synthesizer (Applied Biosystems, Foster City, CA) using Fmoc chemistry and on-line conductivity monitoring during Fmoc deprotection steps. The side chains for Asp, Glu, Ser, and Thr were protected by a *t*-butyl groups, Cys by a trityl group, and Trp and Lys by a *t*-butyloxycarbonyl groups. Preactivation of Fmoc-amino acids was effected by 1:1:2 equiv of *N*-[(dimethylamino)-1*H*-1,2,3-triazolo[4,5-b]pyridin-1-ylmethylene]-*N*-methylmethanaminium hexafluorophosphate *N*-oxide, 1-hydroxy-7-azabenzotriazole (HOAt), and diisopropylethylamine (DIEA) in dimethylformamide and *N*-methylpyrrolidone. The SynthAssist program (Applied Biosystems) was modified to allow the addition of ∼20% DMSO (v/v) to difficult deprotection and coupling reactions. Extended and double coupling reactions were employed for difficult residues. The peptide was deprotected and cleaved from the resin using a standard TFA cleavage protocol in the presence of scavengers (80% TFA:4% H_2O:4% phenol:4% thioanisole:4% ethanedithiol:4% triisopropylsilane). The peptide was extracted by anhydrous ethyl ether, purified on reverse-phase HPLC, and lyophilized. The molecular mass of the peptide was confirmed by plasma desorption mass spectrometry, using a Bioion 20 californium-252 time-of-flight mass spectrometer *(21)*.

Circular Dichroism Analysis of NS3/4A. The far-UV CD spectrum of purified NS3/4A at 0.075 mg/mL was recorded in 10 mM sodium phosphate, pH 8.0, 0.1 M NaCl, and 1 mM dithiothreitol using a Jasco J-500 C spectropolarimeter interfaced with a 486 personal computer. A secondary structure analysis of the resulting spectrum was performed using the program SELCON *(22)*.

State of Aggregation of NS3/4A by Dynamic Light Scattering. Dynamic light scattering experiments on purified NS3/4A were performed in a DynaPro801 (Protein Solution Inc., Charlottesville, VA) instrument at 4 °C. Aliquots of 0.5 mL of the sample in buffer C at 0.5 mg/mL were injected into the instrument inlet through a 0.1 μm on-line filter and the resulting profile was fit by monomodal and bimodal fitting *(23)*.

Assay of NS3/4A Protease Activity. The protease activity of NS3/4A was assayed using the 5AB peptide described above as a substrate. In a typical assay, 50 μM 5AB peptide was incubated with 7 nM NS3/4A for 1 h at 30 °C, which resulted in the cleavage of less than 10% of the substrate. The reaction was quenched by the addition of an equal volume of 1% TFA. The C-terminal, 5B cleavage product was then separated from the substrate and quantified on a Poros 10R2/H reverse-phase column using a PerSeptive Biosystems integral chromatography system and a 10−34% acetonitrile gradient in 0.1% TFA. Except for the time course experiments, all assays were performed in duplicate.

The dependence of product formation on the concentration of NS3/4A between 0.3 and 35 nM was examined by performing the assay in 25 mM Tris, pH 7.5, 0.15 M NaCl, 0.5 mM EDTA, 10% glycerol, 0.05% *n*-dodecyl β-D-maltoside, and 5 mM dithiothreitol.

The pH dependence experiments were performed in 100 mM buffer (MES for pH 4.5, 5.0, 5.5, 6.0, and 6.5; MOPS for pH 6.5 and 7.0; HEPES for pH 7.0 and 7.5; Tris for pH 7.5, 8.0, and 8.5; CHES for pH 8.5, 9.0, and 9.5; CAPS for pH 9.5, 10, and 10.5), 150 mM NaCl, 0.5 mM EDTA, 10% glycerol, 0.05% *n*-dodecyl β-D-maltoside, and 5 mM dithiothreitol. Where buffers of different compositions were tested at the same pH, the protease activity measurements in different buffers at the same pH were within 5% of each other and were averaged to generate Figure 6A. The sodium chloride dependence experiments were performed in 25 mM Tris, pH 8.0, 0.5 mM EDTA, 10% glycerol, 0.05% *n*-dodecyl β-D-maltoside, 5 mM dithiothreitol, and 0−2.0 M NaCl. The glycerol dependence experiments were performed in 25 mM Tris, pH 8.0, 0.3 M NaCl, 0.5 mM EDTA, 0.05% *n*-dodecyl β-D-maltoside, 5 mM dithiothreitol, and 0−50% glycerol. Dithiothreitol dependence experiments were performed in 25 mM Tris, pH 8.0, 0.3 M NaCl, 0.5 mM EDTA, 10% glycerol, 0.05% *n*-dodecyl β-D-maltoside, and 0−10 mM dithiothreitol, using an NS3/4A sample that had been exchanged into the same buffer without dithiothreitol using a Bio-Rad P6 gel-filtration column. The detergent-dependence experiments were performed in 25 mM Tris, pH 8.0,

0.3 M NaCl, 0.5 mM EDTA, 10% glycerol, 5 mM dithiothreitol, and 0−1% detergent (*n*-dodecyl β-D-maltoside, Nonidet P-40, CHAPS, or Tween-20), using an NS3/4A sample that had been exchanged into the same buffer without detergent. EDTA inhibition experiments were performed in 25 mM Tris, pH 8.0, 0.3 M NaCl, 10% glycerol, 0.05% *n*-dodecyl β-D-maltoside, 5 mM dithiothreitol, and 0−100 mM EDTA. Standard protease inhibitors were evaluated in the optimized reaction buffer (25 mM Tris, pH 8.0, 0.3 M NaCl, 0.5 mM EDTA, 10% glycerol, 0.05% *n*-dodecyl β-D-maltoside, and 5 mM dithiothreitol).

In the temperature-dependence experiments, initial rates of 5B product formation were determined at each temperature in the optimized reaction buffer (25 mM Tris, pH 8.0, 0.3 M NaCl, 0.5 mM EDTA, 10% glycerol, 0.05% *n*-dodecyl β-D-maltoside, and 5 mM dithiothreitol), using time courses of 0−120 min at 12 °C, 0−90 min at 15 °C, 0−60 min at 20 °C, 0−45 min at 25 °C, 0−30 min at 30 °C, 0−15 min at 35 °C, and 0−3 min at 40−59 °C.

Determination of NS3/4A Stability at Different Temperatures. NS3/4A at 70 nM was incubated at 12, 25, 30, 37, 45, 50, and 57 °C in the optimized reaction buffer. At each time point, aliquots of NS3/4A were removed and frozen at −80 °C. The NS3/4A samples were later diluted 10-fold to assay their protease activity as described above.

Kinetic Analysis of NS3/4A Protease Activity. A steady-state kinetic analysis of the NS3/4A protease activity was performed in the optimized reaction buffer. NS3/4A (7 nM) was incubated with 2.5−272 μM 5AB substrate for 0−30 min at 30 °C, and the reactions were quenched and quantified as in the 1 h protease assay described above. K_m and V_{max} were obtained from a nonlinear least-squares fit of the data to the Michaelis−Menten equation using the program kΣcat (BioMetallics Inc., Princeton, NJ). The k_{cat} value was calculated from the equation $k_{cat} = V_{max}/[E]$, where [E], the concentration of enzyme, was estimated using the molar extinction coefficient.

Sensitivity of NS3/4A to Protease Inhibitors. A number of commercially available protease inhibitors were screened for inhibition of the NS3/4A protease activity. (The value in parentheses shows the concentration of inhibitor used in the protease assay described above.) (A) Serine protease inhibitors: PMSF (1 mM), Pefabloc (20 mM), benzamidine (10 mM), leupeptin (0.1 mM), antipain (0.1 mM), 3,4-dichloroisocoumarin (0.1 mM), and aprotinin (10 μM). (B) Cysteine protease inhibitor E64 (20 μM). (C) Metalloprotease inhibitors: EDTA (10 mM), bestatin (10 μM), and 1,-10-phenanthroline (5 mM).

State of Aggregation of NS3/4A by Analytical Gel Filtration. Analytical gel filtration was performed on a Pharmacia SMART system using a Superdex Peptide 200 PC 3.2/30 column (Pharmacia) equilibrated with the buffers of the appropriate pH, NaCl concentration, and *n*-dodecyl β-D-maltoside concentration. The composition of these buffers was identical to that of the buffers described under Assay of NS3/4A Protease Activity. Each sample was filtered through a 0.2 μm filter before application onto the column. Samples of purified NS3/4A (50 μL at 0.5 mg/mL) were applied to the column at 50 μL/min. Detection was accomplished spectrophotometrically by absorption at 280 nm.

Assay of NS3/4A ATPase Activity. ATPase assays were performed in a 10 μL reaction volume containing 50 mM HEPES, pH 7.3, 1 mM dithiothreitol, 100 mg/mL BSA, 10 mM $MgCl_2$, and 2.5 mM ATP hot/cold mix containing [α-^{32}P]ATP (3000 Ci/mmol, Amersham). Reactions were carried out in the presence or absence of 1 mM poly(uridylic acid). Assays were incubated for 30 min at 37 °C and terminated by the addition of EDTA to a final concentration of 100 mM. Reaction products were spotted onto a PEI-TLC plastic plate, which was then developed by ascending chromatography in 375 mM potassium phosphate, pH 3.5. Quantitation was accomplished by cutting out the ATP and ADP spots for each reaction on the PEI-TLC sheet and measuring Cherenkov counts using a Packard 2000 CA scintillation counter.

Assay of NS3/4A Helicase Activity. The double-stranded RNA substrate used in the assay was based on the design of Lee and Hurwitz *(24*), except that the two strands overlapped by 21 base pairs and the 3′ overhangs were 15 bases long. The substrate was synthesized by Oligos, Etc. (Wilsonville, OR). The 96-well plates used to measure helicase activity were prepared as follows: Streptavidin-coated 96-well FlashPlates (NEN) were first incubated for 18 h at 25 °C with 250 ng/well of a biotinylated DNA oligomer (capture oligo) complementary to the labeled single-strand RNA of the double-stranded RNA substrate. This reaction occurred in 100 μL/well of buffer containing 25 mM Tris, pH 8.0, 25 mM NaCl, 20% glycerol, and 1 mg/mL BSA. The coated wells were washed three times with 200 μL of PBS.

Helicase reactions were performed in 25 μL reaction mixtures containing 100 mM PIPES, pH 6.0, 1 mM $MgCl_2$, 1 mM ATP, 2 mM dithiothreitol, 1 units of PRIME RNase inhibitor (5 Prime fi 3 Prime, Inc.), 0.1 mg/mL BSA, 250 fmol of double-stranded RNA substrate, and 0−125 fmol of NS3/4A. Mixtures were incubated for 60 min at 37 °C and then 5 μL of 0.5 M EDTA stop solution was added to each reaction, followed by 25 μL of hybridization buffer (1 M NaCl, 50 mM Tris, pH 8.0, and 1 mg/mL BSA). The solution was then transferred to a FlashPlate well coated as described above, and the FlashPlate was incubated for 60 min at 37 °C. Following the hybridization of the released single-stranded RNA to the capture oligomer, reaction mixtures were removed and the wells were washed three times with 200 μL/well of 15 mM NaCl, 1.5 mM sodium citrate, and 1% Tween 20. Assay controls included no-enzyme wells at 37 °C for background calculations and no-enzyme reactions heated to 95 °C for 100% displacement. Plates were read using a Packard 2000 CA Top Count scintillation counter and percent displacement was calculated against the 100% boiled control.

RESULTS

Expression and Purification of NS3/4A. NS3/4A was found to be associated with the insoluble, membrane fraction of Sf9 lysates. A screen of a number of nonionic and zwitterionic detergents demonstrated that 0.5% *n*-dodecyl β-D-maltoside was the most efficient detergent for extraction of active and soluble HisNS3/4A. HisNS3/4A was purified from the detergent extract by Ni−NTA−agarose affinity chromatography (Figure 2, lane 7), yielding 1−4 mg of protein/L of culture. Both HisNS3 (73 kDa) and NS4A (6

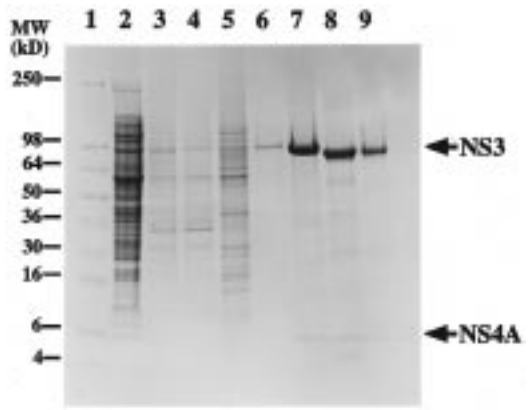

FIGURE 2: SDS−polyacrylamide gel electrophoresis of recombinant NS3/4A at different stages of purification. A 10−20% Tricine minigel (Novex, San Diego, CA) was used under reducing conditions (5% β-mercaptoethanol); 2.5 μg of total protein was loaded in each lane except where otherwise indicated. Lane 1, prestained broad molecular weight standards (Novex); lane 2, total Sf9 lysate (5 μg); lane 3−0.5% *n*-dodecyl β-D-maltoside extract of Sf9 cells; lane 4, Ni−NTA flowthrough; lane 5, Ni−NTA, 25 mM imidazole wash; lane 6, Ni−NTA, 50 mM imidazole wash; lane 7, HisNS3/4A eluted from Ni−NTA column by 250 mM imidazole; lane 8, thrombin-cleaved NS3/4A; lane 9, Superdex-200 purified and concentrated NS3/4A.

kDa) were detected in the sample eluted from the metal chelate column by Coomassie staining (Figure 2) and Western blot (data not shown). No uncleaved HisNS3−4A fusion protein (predicted molecular mass 79 kDa) was detected.

The leader peptide containing the hexahistidine tag was removed from the 73 kD HisNS3 by thrombin cleavage. SDS−PAGE analysis demonstrated that the thrombin cleavage generated a single NS3 species, which had a molecular mass consistent with that of full-length, untagged NS3 (68 kDa) (Figure 2, lane 8). N-Terminal sequencing showed that more than 95% of the cleavage product contained the expected seven heterologous residues (GRRSTSM) at the N-terminus of full-length, natural NS3. Gel filtration of thrombin-cleaved NS3/4A effectively separated the NS3/4A complex from a soluble aggregated form of NS3/4A and from thrombin (Figure 3). NS3 comprised 93% of the total protein in this final preparation, as estimated by scanning a Coomassie-stained SDS−polyacrylamide gel (Figure 2, lane 9) and measuring the intensity of the bands.

The purified NS3/4A complex remained soluble as it was concentrated up to 10 mg/mL, with the concentration based on the extinction coefficient, determined by amino acid analysis, of 66 000 M^{-1} cm^{-1}.

Secondary structure composition of NS3/4A was calculated from its circular dichroism spectrum (data not shown) *(22)* to be 35% α helix and 39% β sheet. These spectrophotometrically determined values are higher than the total amount of regular secondary structure calculated calculated using the Program Procheck *(25)* from the crystal structures of NS3 protease domain complexed with the $NS4A_{21-39}$ peptide *(16)* and of NS3 helicase domain *(17)* combined, which contain approximately 26% α helix and 26% β sheet. This discrepancy suggests that the presence of full-length NS4A in complex with both domains of NS3 may lead to a higher proportion of defined secondary (and possibly tertiary) structure.

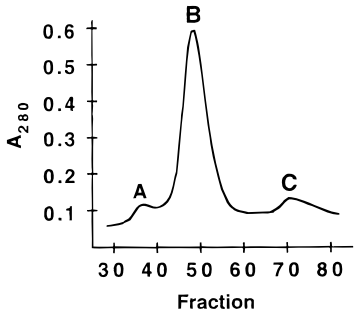

FIGURE 3: Purification of the soluble NS3/4A heterodimer from soluble NS3/4A aggregate and human thrombin by gel filtration. A Superdex 200 (2.6 × 60 cm) column was preequilibrated with 50 mM sodium phosphate, pH 8.0, 0.3 M NaCl, 0.05% *n*-dodecyl β-D-maltoside, 10 mM β-mercaptoethanol, 10% glycerol, 100 ng/mL leupeptin, and 200 ng/mL antipain. Thrombin-cleaved NS3/4A (10 mL) was applied onto the column and run at 2 mL/min. The fractions containing NS3/4A and thrombin were identified by Western blot analysis using α-NS3, α-NS4A, and α-human thrombin primary antibodies. The peaks in the chromatogram correspond to the soluble NS3/4A aggregate (A), soluble NS3/4A heterodimer (B), and human thrombin (C).

Association between NS3 and NS4A. Purification profiles of NS3 and NS4A observed by SDS−PAGE and Western blot analysis, as well as N-terminal peptide sequencing and MALDI mass spectra of the purified sample, all suggest that NS3 and NS4A associate into a noncovalent heterodimer. All through the purification procedure, NS3 and NS4A coeluted from every column as detected by Western blot analysis using antisera against NS3 and NS4A. The molar ratio of the N-termini from NS3 and NS4A in the purified sample was determined by peptide sequencing to be approximately 1.3:1. MALDI mass spectrometric analysis of the NS3/4A protein preparation detected protonated molecular ion MH^+ signals corresponding both to NS3/4A complex and to free NS3 (data not shown).

NS3/4A ATPase and Helicase Activity. NS3/4A displayed poly(uridylic acid)-dependent ATPase activity, which was proportional to the amount of enzyme added (Figure 4A). In the linear range of the assay (0−10 fmol of NS3/4A per reaction), NS3/4A hydrolyzed 0.2 nmol of ATP/fmol of NS3/4A. The helicase activity of NS3/4A on double-stranded RNA substrate was also found to be proportional to the amount of enzyme added (Figure 4B). In the linear range of the assay (0−7.5 fmol of NS3/4A per reaction), NS3/4A unwound 6.5 fmol of the double-stranded substrate/fmol of NS3/4A. Fifty percent displacement of the labeled strand occurred at 30 fmol of the enzyme/reaction.

NS3/4A Protease Activity. A 3 h NS3/4A protease assay performed at 30 °C in 25 mM Tris, pH 7.5, 0.15 M NaCl, 0.5 mM EDTA, 10% glycerol, 0.05% *n*-dodecyl β-D-maltoside, and 5 mM dithiothreitol, using 7 nM NS3/4A and 50 μM 5AB substrate, showed that the initial rate of formation of P′ 5B product increased linearly with time for the first hour. Between 1 and 3 h, the initial rate increasingly deviated from a linear relationship with time (Figure 5A). Since less than 15% of the substrate was converted to product in this experiment, this decrease of protease activity with time was presumed to result from enzyme inactivation.

In 1 h assays under the above reaction conditions, the initial velocity was also found to be linearly proportional to the amount of NS3/4A enzyme added from 0.3 to 35 nM NS3/4A (Figure 5B,C).

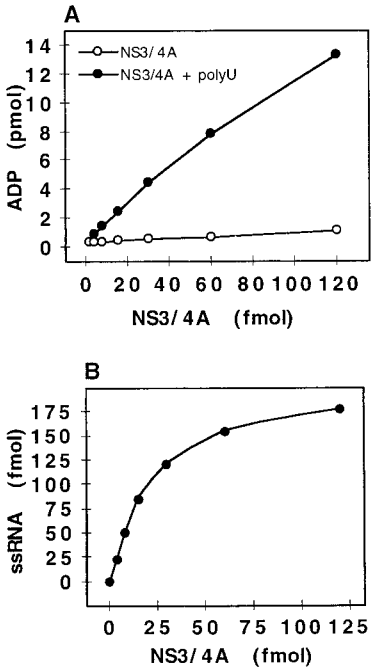

FIGURE 4: NS3/4A ATPase activity (A) and helicase activity (B). The ATPase activity was assayed for 30 min at 37 °C in 50 mM HEPES, pH 7.3, 1 mM dithiothreitol, 100 mg/mL BSA, 10 mM $MgCl_2$, and 2.5 mM ATP hot/cold mix containing [α-^{32}P] ATP (3000 Ci/mmol, Amersham), in the presence (●) or absence (○) of 1 mM poly(uridylic acid). The helicase activity was assayed for 60 min at 37 °C in 100 mM PIPES, pH 6.0, 1 mM $MgCl_2$, 1 mM ATP, 2 mM dithiothreitol, 1 unit of PRIME RNase inhibitor (5 Prime fi 3 Prime, Inc.), and 0.1 mg/mL BSA, with 250 fmol of double-stranded RNA substrate and 0−125 fmol of NS3/4A. The RNA oligonucleotide released from the substrate by the helicase activity was captured on a complementary oligonucleotide immobilized on a FlashPlate and quantified with a scintillation counter.

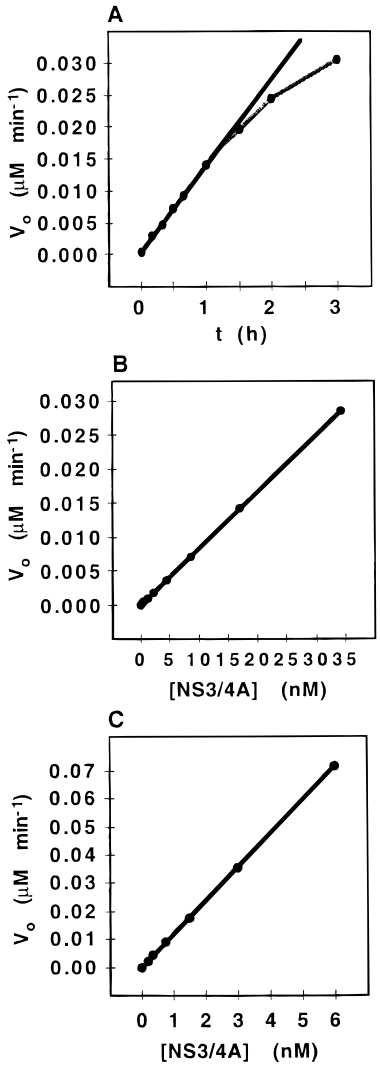

FIGURE 5: Dependence of the initial velocity of NS3/4A protease activity on time (at 7 nM NS3/4A) (A) and concentration of NS3/4A (in a 1 h assay) (B, 0−35 nM NS3/4A; C, 0−6 nM NS3/4A). NS3/4A was incubated with 50 μM 5AB substrate peptide at 30 °C. The assay reaction was stopped by the addition of an equal volume of 1% TFA; the P′ product (5B) peptide was then separated from the substrate (5AB) peptide on a Poros 10R2/H reverse-phase column and quantified by integration of the A_{280} peak against a standard curve.

Protease activity of NS3/4A was sensitive to pH, with a sharp maximum at pH 8.0 (Figure 6A) and a 50% drop in activity with a one-unit change in pH in either direction from the optimal pH. The protease activity was also affected by ionic strength, with a maximal stimulation of 2.5-fold between 0.2 and 0.5 M NaCl (Figure 6B). A further increase of NaCl concentration to 2 M resulted in a gradual decrease of NS3/4A protease activity to approximately 80% of the maximal value. Glycerol was not required for the NS3/4A protease activity. The activity was optimal between 0 and 30% glycerol (Figure 6C) and then dropped by 40% between 30 and 50% glycerol. During the standard 1 h protease assay employed in this study, NS3/4A protease activity was unaffected by the concentration of the reducing agent dithiothreitol between 0 and 10 mM (data not shown).

The nonionic detergent *n*-dodecyl β-D-maltoside in concentrations close to its cmc of 0.01% stimulated the NS3/4A protease activity by approximately 12-fold (Figure 7 A). Nonidet P-40 and Tween 20 were found to stimulate NS3/4A protease activity by a similar amount (data not shown). In contrast, the zwitterionic detergent CHAPS stimulated the protease activity only 2-fold at concentrations approximately half of its cmc and became inhibitory at concentrations above its cmc of 0.5% (Figure 7B).

To examine the effect of temperature on the NS3/4A protease activity, the initial rate of formation of the 5B product was measured at temperatures between 12 and 59 °C. As shown in Figure 8 A, NS3/4A protease activity increased with temperature to a maximum at 40 °C, then decreased at higher temperatures. Below 40 °C, the rate of formation of the 5B product could be measured in the linear range of V_0, which varied between 120 min at 12 °C and 3 min at 40 °C. A comparison of initial rates at such temperatures thus represents a true comparison of protease activity between different temperatures. In contrast, at temperatures ≥45 °C, significant loss of protease activity occurred during the shortest feasible, 3 min time course experiment. Consequently, the initial rates reported for 45 °C and above represent a combination of differences in catalytic efficiency and protein stability.

The effect of prolonged preincubation at different temperatures on the NS3/4A protease activity was also examined. We found that the protease activity decreased with preincubation at ≥25 °C, with a faster decrease at higher temperatures. The half-lives of the NS3/4A protease activity were estimated from the decay curves at each temperature

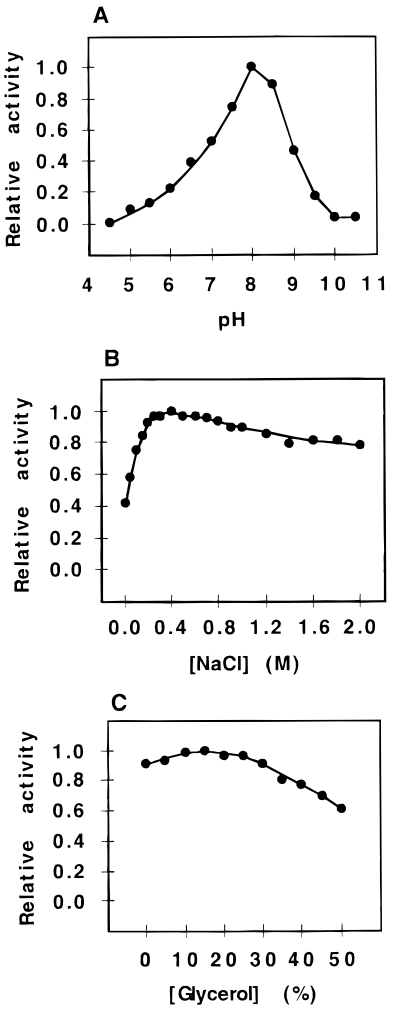

FIGURE 6: Dependence of NS3/4A protease activity on pH (A), concentration of NaCl (B), and concentration of glycerol (C). The pH experiment was performed in 100 mM buffer, 150 mM NaCl, 0.5 mM EDTA, 10% glycerol, 0.05% *n*-dodecyl β-D-maltoside, and 5 mM dithiothreitol. The NaCl experiment was performed in 25 mM Tris, pH 8.0, 0.5 mM EDTA, 10% glycerol, 0.05% *n*-dodecyl β-D-maltoside, and 5 mM dithiothreitol. The glycerol experiment was performed in 25 mM Tris, pH 8.0, 0.3 M NaCl, 0.5 mM EDTA, 0.05% *n*-dodecyl β-D-maltoside, and 5 mM dithiothreitol. Purified NS3/4A (7 nM) was incubated with 50 μM 5AB substrate for 1 h at 30 °C. The amount of 5B product was separated from the substrate and quantified on a reverse-phase column. The initial rates of cleavage under each condition were calculated from the amount of product generated in 1 h, and relative activity was calculated by dividing each initial rate by the highest initial rate obtained in each experiment. All experiments were performed in duplicate, with the variation between duplicate 5B product concentrations between 0.1, and 5% of the total concentration.

(Figure 8B). The 30-fold increase of the half-life from 37 to 30 °C reinforced the choice of 30 °C as the temperature for the assay of NS3/4A protease activity.

NS3/4A protease activity with the 5AB peptide substrate at 30 °C conformed to simple Michaelis−Menten kinetics (Figure 9). Under the optimized buffer conditions, the NS3/4A protease activity was shown to be associated with the following apparent kinetic constants: $K_m = 59 (\pm 3)$ μM, $V_{max} = 0.058 (\pm 0.001)$ μM/min, $k_{cat} = 0.22 (\pm 0.02)$ s^{-1}, and $k_{cat}/K_m = 3700 (\pm 600)$ s^{-1} M^{-1}.

Of the commercially available protease inhibitors tested, the irreversible serine protease inhibitor Pefabloc and known metalloprotease inhibitors EDTA and 1,10- phenanthroline

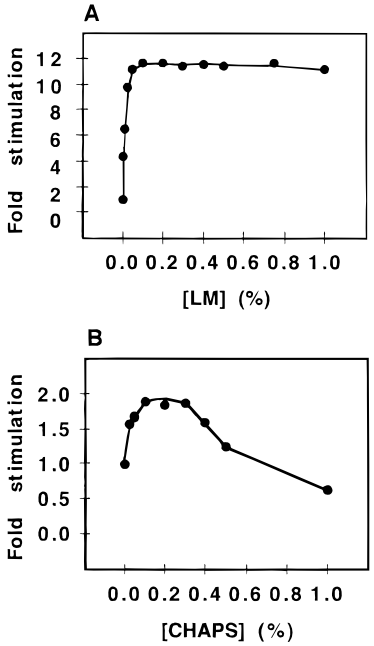

FIGURE 7: Stimulation of NS3/4A protease activity by *n*-dodecyl β-D-maltoside (A) and CHAPS (B). The detergent titrations were performed in 25 mM Tris, pH 8.0, 0.3 M NaCl, 0.5 mM EDTA, and 5 mM dithiothreitol.

inhibited NS3/4A protease activity. The IC_{50}s for these three inhibitors were found to be 7 mM, 10 mM, and 12 mM, respectively (data not shown).

State of Aggregation of NS3/4A. In this study we found that NS3/4A existed in three possible states of aggregation: (A) soluble, nonaggregated, monodisperse, NS3/4A heterodimer (soluble heterodimer, SH); (B) soluble, polydisperse, NS3/4A aggregate (soluble aggregate, SA), with molecular mass of $\geq$500 kDa, which remained in solution after ultracentrifugation at 100000*g* (data not shown) and could be dissociated into soluble heterodimer by the addition of more nonionic detergent; and (C) Insoluble NS3/4A aggregate (insoluble aggregate, IA), which could be removed from solution by ultracentrifugation at 100000*g* or by filtration through a 0.2 μm filter.

The two soluble forms were separated by gel filtration on an analytical Superdex 200 column. The soluble heterodimer chromatographed in the included volume, exhibiting apparent molecular mass of $\leq$200 kDa, whereas the soluble aggregate was eluted in the void volume. In contrast, the insoluble aggregate was removed from the sample by filtration before the sample was loaded onto the Superdex-200 column.

In the studies of the effect of the detergent *n*-dodecyl β-D-maltoside on the state of aggregation of NS3/4A at pH 8.0 and 0.3 M NaCl, NS3/4A was found to be soluble and to distribute between soluble heterodimer and soluble aggregate. The proportion of soluble heterodimer in the mixture increased sharply from 0 to 90% between 0.005% and 0.01% *n*-dodecyl β-D-maltoside (Figure 10 C) and then remained the same at higher concentrations of the detergent.

In the studies of the effect of pH and salt on the state of aggregation of NS3/4A, NS3/4A was found to distribute between the soluble heterodimer and the insoluble aggregate. No soluble heterodimer was detected between pH 5 and 6. The amount of soluble heterodimer increased with pH from 6 to 8 and then remained high between pH 8 and 10 (Figure

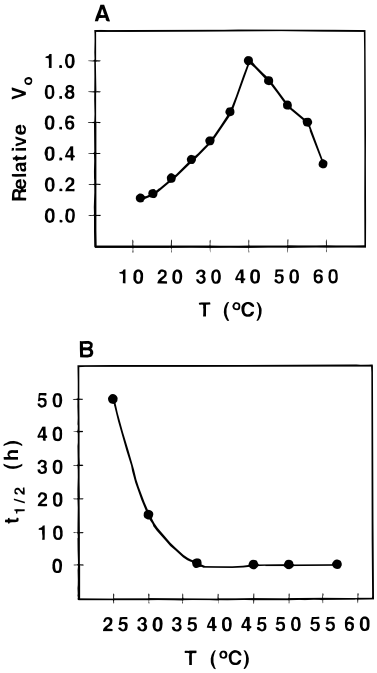

FIGURE 8: (A) Temperature dependence of NS3/4A protease activity. Initial rates of 5B product formation were determined at each temperature, using time courses of 0−120 min at 12 °C, 0−90 min at 15 °C, 0−60 min at 20 °C, 0−45 min at 25 °C, 0−30 min at 30 °C, 0−15 min at 35 °C, and 0−3 min at 40−59 °C. (B) Temperature dependence of the half-life of NS3/4A protease activity. NS3/4A samples (70 nM) were preincubated at each temperature. Aliquots were removed from the samples at different times and diluted 10-fold into 25 mM Tris, pH 8.0, 0.3 M NaCl, 0.5 mM EDTA, 10% glycerol, 0.05% *n*-dodecyl β-D-maltoside, and 5 mM dithiothreitol with 50 μM 5AB substrate. The protease assays were performed for 30 min at 30 °C. The curves summarizing the decay of protease activity with time were used to estimate the half-life ($t_{1/2}$) of the activity at each temperature. The half-lives were found to be 50 h at 25 °C, 15 h at 30 °C, 30 min at 37 °C, 10 min at 45 °C, 4 min at 50 °C, and 1.5 min at 57 °C.

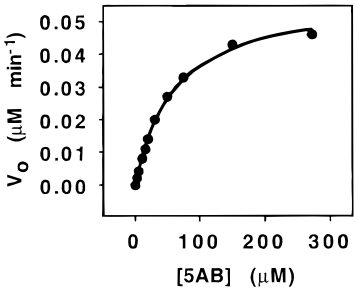

FIGURE 9: Kinetic analysis of NS3/4A protease activity in 25 mM Tris, pH 8.0, 0.3 M NaCl, 0.5 mM EDTA, 10% glycerol, 0.05% *n*-dodecyl β-D-maltoside, and 5 mM dithiothreitol. NS3/4A (7 nM) was incubated with 2.5−272 μM 5AB substrate for 0−30 min at 30 °C. Curve-fitting to the Michaelis−Menten equation was done using the k•cat program (BioMetallics, Inc., Princeton, NJ). The resulting kinetic constants are K_m = 59 (± 3) μM, V_{max} = 0.058 (± 0.001) μM/min, k_{cat} = 0.22 (± 0.03) s^{-1}, and k_{cat}/K_m = 3700 (± 600) M^{-1} s^{-1}).

10A). Similarly, the amount of soluble heterodimer increased with the concentration of NaCl from 0 to 0.3 M and then remained at the same level at 1 M (Figure 10B).

Dynamic light scattering studies of purified NS3/4A in 0.05% *n*-dodecyl β-D-maltoside revealed two distinct peaks in particle size distribution (data not shown). The distribution between the two peaks was consistent with a monodisperse sample when fit with the bimodal approach. The major peak

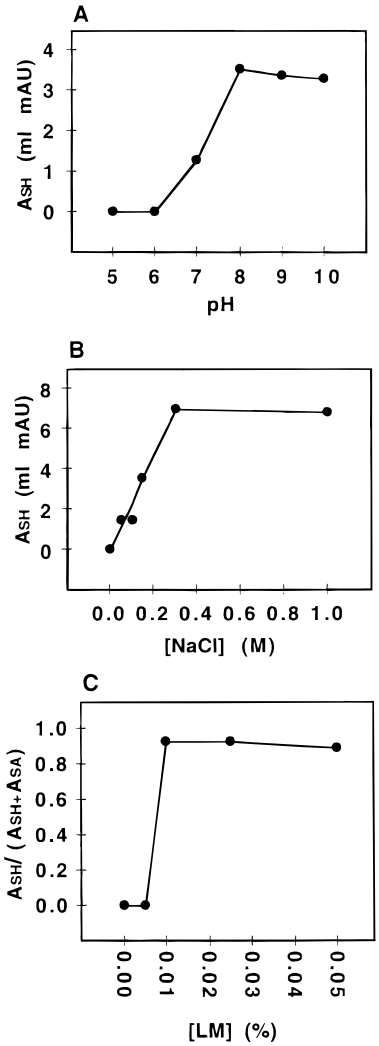

FIGURE 10: Effect of pH (A), concentration of NaCl (B), and concentration of *n*-dodecyl β-D-maltoside (C) on the aggregation state of NS3/4A. Purified NS3/4A (50 μL at 0.5 mg/mL) was filtered to remove any insoluble aggregate and then loaded onto an analytical Superdex-200 PC 3.2/20 column that had been equilibrated with the sample buffer. The column was run at 50 μL/min to separate the soluble heterodimer from any soluble aggregate. In the cases of pH and NaCl titration, any NS3/4A not present as soluble heterodimer had aggregated and had been removed from the sample by filtration; the peak areas plotted in panels A and B thus represent the total amount of soluble heterodimer included in the column bed. In the case of *n*-dodecyl β-D-maltoside titration, on the other hand, NS3/4A was distributed between soluble heterodimer and soluble aggregate. Consequently, the value plotted in panel C represents the proportion of total NS3/4A present in the form of soluble heterodimer. A, peak area; SH, soluble heterodimer; SA, soluble aggregate.

(> 95% of protein population) contained protein of a particle size consistent with the predicted molecular mass of NS3/4A, and the minor peak (<5% of protein population) contained protein with a particle size of over 500 kDa. In the absence of 0.05% *n*-dodecyl β-D-maltoside, dynamic light scattering revealed a polydisperse sample, with all the particles larger than 500 kDa.

DISCUSSION

Using an Sf9/baculovirus expression system, we expressed and purified to homogeneity the full-length HCV NS3 protease and its NS4A activator. The genes for NS3 and

NS4A were cloned in tandem, downstream from a sequence encoding a leader peptide that contained a hexahistidine tag. We found that the HisNS3/4A complex was processed in the Sf9 cells at the natural cis cleavage site between the two proteins, resulting in the HisNS3 and NS4A proteins of the expected molecular masses. This was the first indication that the NS3/4A construct had the expected protease activity and specificity in vivo. The NS3/4A was found in the insoluble fraction of cell lysate, which is consistent with the previous findings that NS4A directs NS3 to the cell membrane *(26)*. We extracted NS3/4A from the membrane fraction and solubilized it using the nonionic detergent *n*-dodecyl β-D-maltoside. NS3 and NS4A copurified throughout the purification procedure, which consisted of metal chelate affinity chromatography, removal of the leader peptide by thrombin cleavage, and gel-filtration chromatography. N-Terminal protein sequencing and MALDI mass spectrometry demonstrated that the final, 93% pure preparation of NS3/4A contained the two proteins in nearly equimolar amounts. The above observations lead us to believe that NS3 and NS4A exist in solution as a noncovalently bound complex. The persistence of this complex under reducing conditions suggests that no essential intermolecular disulfide bonds are involved in the stabilization of the complex.

It has been shown that the presence of NS4A enhances the activity of the NS3 protease *(11, 14)*. Consequently, the fact that the protease activity of the NS3/4A complex is linearly dependent on the concentration of the complex down to the detection limit of 0.3 nM NS3/4A (Figure 5C) suggests that the dissociation constant of NS3 and NS4A is less than 0.1 nM. This is not surprising given the crystal structure of the complex between NS3 protease domain and NS4A-derived peptide *(26)*, where $NS4A_{21-39}$ makes up one of the strands of the antiparallel β sheet of the NS3 protease domain. The intercalation of NS3 and NS4A raises the question of whether we should consider NS4A as a separate protein essential for the activation of the NS3 protease or whether we should look upon NS3/4A as a single protein which happens to cleave one of its own loops. The third possibility is that the NS3/4A before autoprocessing is a proenzyme that needs to be cleaved at the junction between NS3 and NS4A in order to be activated. This question may be resolved once a crystal structure of full-length NS3/4A complex has been solved and the enzymology of uncleavable mutants of NS3/4A is examined.

The purified NS3/4A complex exhibited protease activity, poly(uridylic acid)-dependent ATPase activity, and helicase activity. The detailed characterization of the ATPase and helicase activity will be reported elsewhere (Chase et al., manuscript in preparation). In this report, we focus on the characterization of the NS3/4A protease activity and its relationship to the aggregation state. Protease activity was measured using a synthetic peptide substrate (P8P8′K) derived from the NS5A−NS5B junction in the HCV(1a) precursor polyprotein. The choice of the substrate was governed by the work of Zhang et al. *(27)*, which demonstrated that the NS5A−NS5B-derived peptide was cleaved more efficiently than comparable peptides derived from the NS4A−NS4B or NS4B−NS5A junction.

Under most conditions we find that the dependence of NS3/4A protease activity on pH, concentration of NaCl, and concentration of *n*-dodecyl β-D-maltoside correlates closely with the effect of these conditions on the NS3/4A state of aggregation. The highest protease activity is seen under the conditions where NS3/4A is in the form of a soluble, nonaggregated, monodisperse complex of NS3 and NS4A. Lower NS3/4A protease activity is observed under conditions where NS3/4A is even partially in the form of a soluble aggregate, such as at suboptimal concentrations of *n*-dodecyl β-D-maltoside, or in the form of insoluble aggregate, such as at suboptimal pH or suboptimal concentration of NaCl. The exception to the above correlation between protease activity and state of aggregation occurs when the pH is above the activity optimum of 8.0. In this region of high pH, NS3/4A does not aggregate during the 2 h gel-filtration experiment, but it is nevertheless less active, with a drop in activity of 50% between pH 8.0 and 9.0.

Under buffer conditions where NS3/4A protease activity inversely correlates with its aggregation state, we interpret the differences in protease activity in terms of availability of monodisperse NS3/4A heterodimer rather than in terms of the chemical environment at the active site. Similarly, the loss of activity above pH 8.5 can be attributed to the ionization of cysteine residues close to their pK_a, followed by changes in the electrostatic environment both in the NS3/4A molecule and in the peptide substrate.

The steady-state kinetic constants of NS3/4A protease activity under optimal buffer conditions are $K_m = 59$ ($\pm$ 3) μM, $V_{max} = 0.058$ ($\pm$ 0.001) μM/min, $k_{cat} = 0.22$ ($\pm$ 0.03) s^{-1}, and $k_{cat}/K_m = 3700$ ($\pm$ 600) s^{-1} M^{-1}. The catalytic efficiency of NS3/4A is an order of magnitude higher than has been reported for the $NS3_{1-180}$ protease domain with synthetic $NS4A_{21-35}$ peptide ($k_{cat}/K_m = 648$ M^{-1} s^{-1}) *(28)* and for a maltose-binding protein fusion of $NS2_{126-200}$−$NS3_{1-589}$ with synthetic $NS4A_{18-40}$ peptide ($k_{cat}/K_m = 255$ M^{-1} s^{-1}) *(29)*. The difference in protease activity between the full-length NS3/4A expressed in baculovirus and the previously published constructs is more pronounced in the k_{cat} values [previously reported as 0.01 s^{-1} *(28)* and 0.03 s^{-1} *(29)*] than in the K_m values [previously reported as 30 μM *(28)* and 108 μM *(29)*]. This pattern suggests that the affinity of NS3 for its substrates changes little when different parts of NS3/4A are present in addition to the minimal protease and NS4A activating domains but that the full-length enzyme is more efficient at cleaving the substrate than are its smaller domains. The N-terminal and C-terminal ends of NS4A may well have a role in the structure and function of full-length NS3 protease that cannot be reproduced by the central hydrophobic stretch of NS4A alone.

The screening of a range of standard serine protease inhibitors revealed irreversible inhibition of NS3/4A protease activity by Pefabloc, which is consistent with the essentiality of the active-site serine in catalysis *(30−32)*. On the other hand, the lack of inhibition of NS3/4A protease activity by a number of commonly available serine inhibitors suggests that the HCV serine protease has a unique active-site environment, which may lend itself to the design of highly selective inhibitors. The two weak metal protease inhibitors of NS3/4A are metal chelators, which probably exert their effect by binding the structural zinc seen in the crystal structures of the protease domain *(15, 16)* and thus destabilizing the native structure of the protein.

In summary, we show here that the full-length NS3/4A is more soluble and active than the earlier constructs containing a combination of NS3 domains and NS4A-derived peptides. A three-dimensional structure of the NS4/4A complex is needed to examine the interactions of the N-terminal NS3 protease domain with the C-terminal NS3 ATPase/helicase domain, the full-length NS4A, and the cell membrane.

ACKNOWLEDGMENT

We thank Dr. Jeffrey L. Schwartz and Mr. Joseph J. Troyanovich for the fermentation support, Mr. Jim Durkin for the synthesis and purification of the peptide substrate, Dr. William Windsor for helpful discussion and peptide chemistry support, and Dr. U. Bahr (University of Frankfurt, Germany) for her help with the MALDI mass spectrometry analysis.

REFERENCES

1. Houghton, M., Weiner, A., Han, J., Kuo, G., and Choo, Q.-L. (1991) *Hepatology 14,* 381−388.
2. Bruix, J., Cavalet, X., Costa, J., Ventura, M., Bruguera, M., Castillo, R., Barrera, J. M., Ercilla, G., Sanchez-Tapias, J. M., Vall, M., Bru, C., and Rodes, J. (1989) *Lancet ii,* 1004−1006.
3. Weiland, O. (1994) *FEMS Microbiol. Rev. 14,* 279−288.
4. Choo, Q.-L., Kuo, G., Weiner, A. J., Bradley, L. R. D. W., and Houghton, M. (1989) *Science 244,* 359−362.
5. Kato, N., Hijikata, M., Ootsuyama, Y., Nakagawa, M., Ohkoshi, S., Sugimura, T., and Shimotohno, K. (1990) *Proc. Natl. Acad. Sci. U.S.A. 87,* 9524−9528.
6. Inchauspe, G., Zebedee, S., Lee, D.-H., Sugitani, M., Nasoff, M., and Prince, A. M. (1991) *Proc. Natl. Acad. Sci. U.S.A. 88,* 10292−10296.
7. Takamizawa, A., Mori, C., Fuke, I., Manabe, S., Murakami, S., Fujita, J., Onishi, E., Andoh, T., Yosha, I., and Okayama, H. (1991) *J. Virol. 65,* 1105−1113.
8. Tsukiyama-Kohara, K., Kohara, M., Yamaguchi, K., Maki, N., Toyoshima, A., Miki, K., Tanaka, S., Hattori, N., and Nomoto, A. (1991) *Virus Genes 5,* 243−254.
9. Francki, R. I. B., Fauquet, C. M., Knudson, D. L., and Brown, F. (1991) *Arch. Virol. 2* (Suppl.), 223.
10. Hijikata, M., Kato, N., Ootsuyama, Y., Nakagawa, M., and Shimotohno, K. (1991) *Proc. Natl. Acad. Sci. U.S.A. 88,* 5547−5551.
11. Grakoui, A., McCourt, D. W., Wychowski, C., Feinstone, S. M., and Rice, C. (1993) *Proc. Natl. Acad. Sci. U.S.A. 90,* 10583−10587.
12. Jin, L., and Peterson, D. L. (1995) *Arch. Biochem. Biophys. 323,* 47−53.
13. Kim, D. W., Gwack, Y., Han, J. H. and Choe, J. (1995) *Biochem. Biophys. Res. Commun. 215,* 160−166.
14. Failla, C., Tomei, L., and De Francesco, R. (1994) *J. Virol. 68,* 3753−3760.
15. Love, R. A., Parge, H. E., Wickersham, J. A., Hostomsky, Z., Habuka, N., Moomaw, E. W., Adachi, T., and Hostomska, Z. (1996) *Cell 87,* 331−342.
16. Kim, J. L., Morgenstern, K. A., Lin, C., Fox, T., Dwyer, M. D., Landro, J. A., Chambers, S. P., Markland, W., Lepre, C. A., O'Malley, E. T., Habeson, S. L., Rice, C. M., Murcko, M. A., Caron, P. R., and Thomson, J. A. (1996) *Cell 87,* 343−355.
17. Yao, N., Hesson, T., Cable, M., Hong, Z., Kwong, A. D., Le, H. V., and Weber, P. (1997) *Nat. Struct. Bio. 4,* 463−467.
18. Morgenstern, K. A., Landro, J. A., Hsiao, K., Lin, C., Gu, Y., Su, M. S.-S., and Thomson, J. A. (1997) *J. Virol. 71,* 3767−3775.
19. Hong, Z., Ferrari, E., Wright-Minogue, J., Chase, R., Risano, C., Seelig, G., Lee, C.-G., and Kwong, A. D. (1996*) J. Virol. 70,* 4261−4268.
20. Tsarbopoulos, A., Karas, M., Strupat, K., Pramanik, B., Nagabhushan, T. L., and Hillenkamp, F. (1994) *Anal. Chem. 66,* 2062−2070.
21. Tsarbopoulos, A., Becker, G. W., Occolowitz, J. L., and Jardine, I. (1988) *Anal. Biochem. 171,* 113−123.
22. Sreerama, N., and Woody, R. W. (1993) *Anal. Biochem. 209,* 32−44.
23. Ostrowsky, N., Sornette, D., Parker, P., and Pike, E. R. (1981) *Opt/ Acta 28,* 1059−1070.
24. Lee, C.-G., and Hurwitz, J. (1992*) J. Biol. Chem. 262,* 4398−4407.
25. Laskowski, R. A., Rullmann, J. A. C., MacArthuyr, M. W., Kaptein, R., and Thornton, J. M. (1996) *J. Biomol. NMR 8,* 477−486.
26. Satoh, S., Tanji, Y., Hijikata, M., Kimura, K., and Shimotohno, K. (1995) *J. Virol. 69,* 4355−4360.
27. Zhang, R., Durkin, J., Windsor, W. T., McNemar, C., Ramanathan, L., and Le, H. V. (1997) *J. Virol. 71,* 6208−6213.
28. Steinkuhler, C., Tomei, L., and De Francesco, R. (1996) *J. Biol. Chem. 271,* 6367−6373.
29. Shimizu, Y., Yamaji, K., Masuho, Y., Yokota, T., Inoue, H., Satoh, S., and Shimotohno, K. (1996) *J. Virol. 70,* 127−132.
30. Bartenschlager, R., Ahlborn-Laake, L., Mous, J., and Jacobsen, H. (1993) *J. Virol. 67,* 3835−3844.
31. Grakoui, A., McCourt, D. W., Wychowski, C., Feinstone, S. M., and Rice, C. (1993) *J. Virol. 67,* 2832−2843.
32. Tomei, L., Failla, C., Santolini, E., de Francesco, R., and La Monica, N. (1993) *J. Virol. 67,* 4017−4026.

BI972010R